Nuclear Engineering and Technology 54 (2022) 959–964

Contents lists available at ScienceDirect

Nuclear Engineering and Technology

journal homepage: www.elsevier.com/locate/net

Original article

Validation of the neutron lead transport for fusion applications

Martin Schulc*, Michal Košťál, Evžen Novák, Tomáš Czakoj, Jan Šimon

Research Centre Rez Ltd, 250 68 Husinec-Řež 130, Czech Republic

ARTICLE INFO

Article history:
Received 10 May 2021
Received in revised form
18 August 2021
Accepted 2 September 2021
Available online 7 September 2021

Keywords:
Lead cross sections
^{252}Cf
ENDF/B-VIII.0
Tritium breeding ratio
Lithium-lead modules
IRDFF-II

ABSTRACT

Lead is an important material, both for fusion or fission reactors. The cross sections of natural lead should be validated because lead is a main component of lithium-lead modules suggested for fusion power plants and it directly affects the crucial variable, tritium breeding ratio. The presented study discusses a validation of the lead transport libraries by dint of the activation of carefully selected activation samples. The high emission standard ^{252}Cf neutron source was used as a neutron source for the presented validation experiment. In the irradiation setup, the samples were placed behind 5 and 10 cm of the lead material. Samples were measured using a gamma spectrometry to infer the reaction rate and compared with MCNP6 calculations using ENDF/B-VIII.0 lead cross sections. The experiment used validated IRDFF-II dosimetric reactions to validate lead cross sections, namely ^{197}Au(n, 2n)^{196}Au, ^{58}Ni(n,p)^{58}Co, ^{93}Nb(n, 2n)^{92m}Nb, ^{115}In(n,n')^{115m}In, ^{115}In(n,γ)^{116m}In, ^{197}Au(n,γ)^{198}Au and ^{63}Cu(n,γ)^{64}Cu reactions. The threshold reactions agree reasonably with calculations; however, the experimental data suggests a higher thermal neutron flux behind lead bricks. The paper also suggests ^{252}Cf isotropic source as a valuable tool for validation of some cross-sections important for fusion applications, i.e. reactions on structural materials, e.g. Cu, Pb, etc.

1. Introduction

Lead is an important material. Lead is a main component of lithium-lead tritium breeding modules suggested for tritium breeding in fusion power plants. Thus, it is very reasonable to verify neutron lead cross sections. The way to reach the goal to get the correct cross sections evaluations is complicated by the fact that it is composed of four stable isotopes, and their content differs. The ^{252}Cf was chosen as a neutron source since it is the only neutron standard with the lowest uncertainties in the neutron spectrum possible. Fusion sources are not reference or standard neutron fields, so their input neutron spectra are necessarily loaded with higher uncertainty. From this point of view, ^{252}Cf source is a preferable tool for validation. It is important to validate transport cross sections by validated cross sections. If the reaction rate does not agree with experiment, transport cross sections cannot be correct. If transport is not correct, then tritium breeding ratio cannot be estimated correctly.

The Helium-Cooled Lithium–Lead (HCLL) blanket concept is one of the main research lines using lead in breeding modules considered in the European Fusion Technology Programme for DEMO fusion reactor. The HCLL blanket uses ferritic steel Eurofer as a structural material, Pb–17Li eutectic alloy as a tritium breeder and neutron multiplier, and helium as a coolant [1]. Other concepts containing lead are Water-Cooled Lithium–Lead (WCLL) and dual coolant lithium-lead breeding (DCLL) blankets. Technical details of all of these concepts can be found in Ref. [2].

Neutron HCLL spectra in benchmarks are calculated in complex models. They use cross sections which need to be validated in calculations. ^{252}Cf is an independent standard source, its spectrum does not depend on calculations. The uncertainty in HCLL benchmark input spectra are higher than 10% but for Cf-252 it is around 1%. It is crucial for correct tritium breeding ratio.

All of the blanket concepts are loaded with high design uncertainties, so it is crucial to perform experiments that can be used to lower these uncertainties. Generally, there is a lack of experiments concerning neutron transport through lead for fusion applications. One of these experiments is presented in this manuscript. We focused on activation analysis including radiative capture and threshold reactions. The authors of the comprehensive paper concerning neutronics and tritium breeding ratio inside HCLL mock-up [3] also performed activation analysis for threshold reactions. More recently, a lead benchmark experiment with DT Neutrons was performed at JAEA/FNS facility [4].

* Corresponding author.
E-mail address: martin.schulc@cvrez.cz (M. Schulc).

https://doi.org/10.1016/j.net.2021.09.002

Table 1
Isotopic composition of lead in %.

	^{204}Pb	^{206}Pb	^{207}Pb	^{208}Pb
Range of natural variation	1.04–1.65	20.84–27.48	17.62–23.65	51.28–56.21
Representative values	1.4	24.1	22.1	52.4

2. Experimental setup

The ^{252}Cf isotopic neutron source was selected as a source of neutrons, as the ^{252}Cf spontaneous fission neutron spectrum is the only neutron standard, so it is a suitable tool for validation. The ^{252}Cf source had an average total emission of 2.31E8 n/s during irradiation. The emission was derived from the data in the Certificate of Calibration obtained from the National Physical Laboratory, United Kingdom using exponential decay law. More details concerning the use of the source for precise experiments and uncertainty analysis for used neutron source can be found in [18]. The relevant experimental uncertainties that have been investigated in this experimental setup were: uncertainties on the experimental positions of the samples, lead density, emission of the source, the net peak area uncertainties measured by the HPGe detector and the detector efficiency uncertainty. Natural lead is composed of four isotopes ^{204}Pb, ^{206}Pb, ^{207}Pb, and ^{208}Pb. Unfortunately, the isotopic composition varies with different samples. Table 1 shows the range of the isotopic variation of the lead isotopes [5]. Representative values were picked for the calculation [5]. Sensitivity analysis concerning the influence of individual isotopes was performed to take into account the dispersion of the isotopic content. The conservative approach was employed into the sensitivity analysis, i.e. the reaction rates were calculated for minimal and maximal values of the parameter under study.

The lead bricks are composed of natural lead (97.2%) and 2.5% of antimony according to the XRF analysis. The rest is composed of Rhenium, Calcium, Iron, baryum and Cesium. The source was centred and placed just behind the lead wall according to Fig. 1. The lead wall was composed of two rows of lead bricks. The thickness of the one lead brick is 5 cm, the wall was 10 cm thick. The height and width of the wall were 52.5 cm both. The activation foils (for a list of reactions, see Table 2) were attached to the wall using thin 0.06 cm thin aluminium foil, see Fig. 2. These foils were divided into two packs, one pack was put behind the first wall of bricks (5 cm of lead), and the second pack was placed in the middle just behind the second row of the bricks. The masses of activation foils vary from 0.4 g (Cu) to 5 g (Nb). The thickness of activation foils was 1 mm at most (Nb). The irradiation lasted 26.7 days continuously.

At the end of the irradiation, all irradiated samples were placed on the upper cap of the high purity germanium HPGe detector ORTEC GM35P4 one by one. The distance between sample and Germanium crystal was 0.65 cm. The detector efficiency was directly calculated using a MCNP6.2 [6] model based on the experimentally measured dimensions, see Ref. [7]. The experimental reaction rate q was computed using the following formula

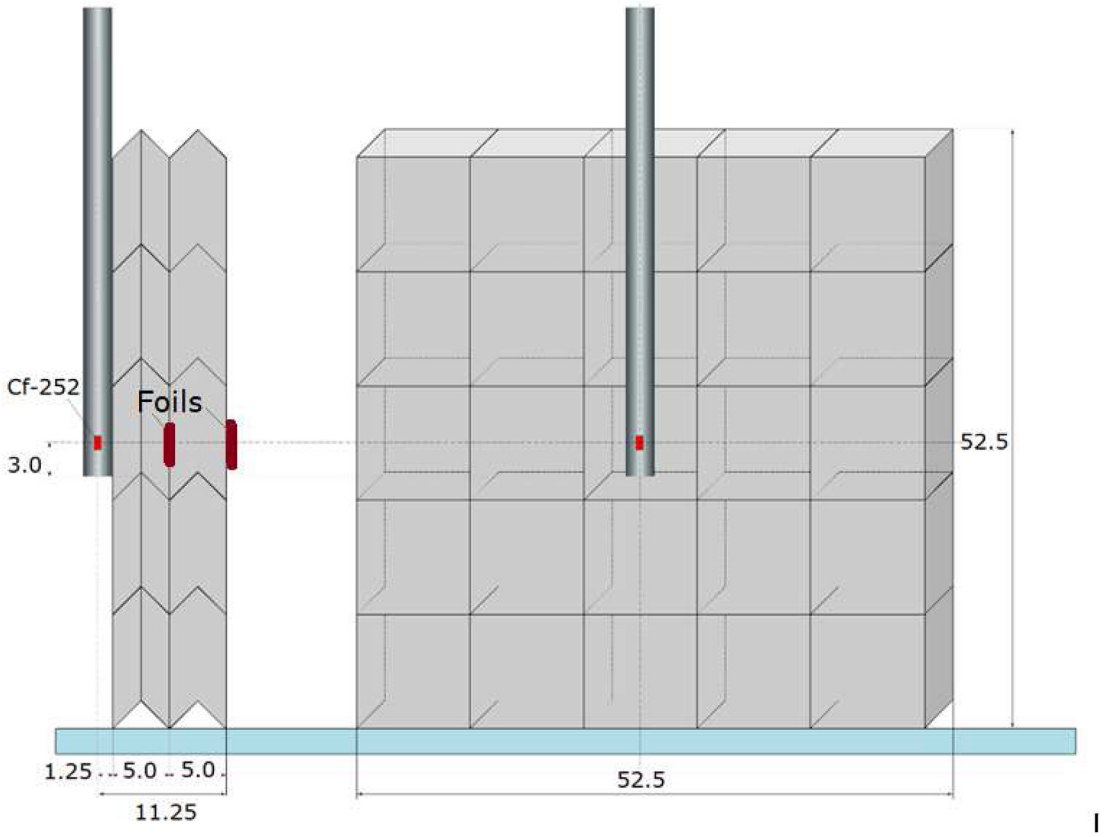

Fig. 1. Cross section side and front view of the lead configuration. The neutron source was placed just behind the lead wall, into its centre. All dimensions are displayed in centimetres.

Table 2
Parameters of the investigated neutron-induced threshold reactions.

Reaction	Half-life	Gamma Energy [MeV]	Gamma absolute intensity
^{197}Au(n,γ)^{198}Au	2.6941 days	0.41180205	0.9562
^{197}Au(n,2n)^{196}Au	6.1669 days	0.35573	0.87
^{63}Cu(n,γ)^{64}Cu	12.701 h	0.5110	0.352
^{58}Ni(n,p)^{58}Co	70.86 days	0.8107593	0.9945
^{93}Nb(n,2n)^{92m}Nb	10.15 days	0.93444	0.9915
^{115}In(n,n')^{115m}In	4.486 h	0.336241	0.459
^{115}In(n,γ)^{116m}In	54.29 min	1.29356	0.848

$$q = \frac{C(T_m)\lambda T_m}{\eta\varepsilon N K T_l}\,\frac{1}{e^{-\lambda \Delta T}}\,\frac{1}{1-e^{-\lambda T_m}}\,\frac{1}{1-e^{-\lambda T_{irr}}}, \quad (1)$$

where: q is the experimental reaction rate per atom per second, N is the number of target isotope nuclei, η is the detector efficiency, ε is the gamma absolute intensity, λ is the decay constant, k characterizes the abundance of the isotope of interest in the target and its purity, ΔT is the time between the end of irradiation and the start of spectrometry measurement, $C(T_m)$ is the net peak area, T_m is the real time of measurement by HPGe, T_l is the live time of measurement by HPGe (it is time of measurement corrected to the dead time of the detector), and T_{irr} is the time of irradiation.

Table 2 summarizes the measured activation products parameters, i.e. half-life, gamma transition energy used for analysis, and gamma absolute intensity. Table 3 shows gamma spectroscopy parameters, irradiation time, cooling times, and subsequent HPGe measurement times for all activation products.

Table 3
Parameters of irradiation and following gamma spectrometry measurement.

Reaction	Irradiation time	Cooling time	Measurement time
^{197}Au(n,γ)^{198}Au	26.7 days	3.26 h, 23.23 h	19.9 h, 5.64 h
^{197}Au(n,2n)^{196}Au	26.7 days	3.26 h, 23.23 h	19.9 h, 5.64 h
^{63}Cu(n,γ)^{64}Cu	26.7 days	69.32 min	2.15 h
^{58}Ni(n,p)^{58}Co	26.7 days	7.90 days	7.23 h
^{93}Nb(n,2n)^{92m}Nb	26.7 days	1.21 days	1.85 days
^{115}In(n,n')^{115m}In	26.7 days	26.43 min	41.85 min
^{115}In(n,γ)^{116m}In	26.7 days	26.43 min	41.85 min

3. Calculations

Calculations of reaction rates were performed by means of the f4 tallies (average flux in a cell of interest) in MCNP6.2 transport code using ENDF/B-VIII.0 neutron transport library for lead [8]. Calculations in other transport libraries i.e. ENDF/B-VII.1 [9] and JEFF-3.3 [10] gave similar results as ENDF/B-VIII.0. Evaluations have only slight differences, mainly in resonance region and angular distributions. These differences had not influence on our results within uncertainties. For this reason, only results in ENDF/B-VIII.0 transport library are shown.

The cross sections of reactions investigated in this experiment were taken from dosimetric IRDFF-II [11] library. The IAEA recommended input ^{252}Cf spontaneous fission neutron spectrum [12] was used for all calculations. The whole geometry including activation foils was included in the MCNP6.2 model. The model takes into account all available data (dimensions, densities, materials …) which were precisely measured with uncertainty around 1%. The walls of lab were included in the computational model.

4. Results

Fig. 3 demonstrates the cross sections of all investigated dosimetric reactions plus tritium breeding crucial ^{6}Li(n,T)^{4}He reaction

Fig. 2. Lead bricks configuration containing activation foils holder made of aluminium.

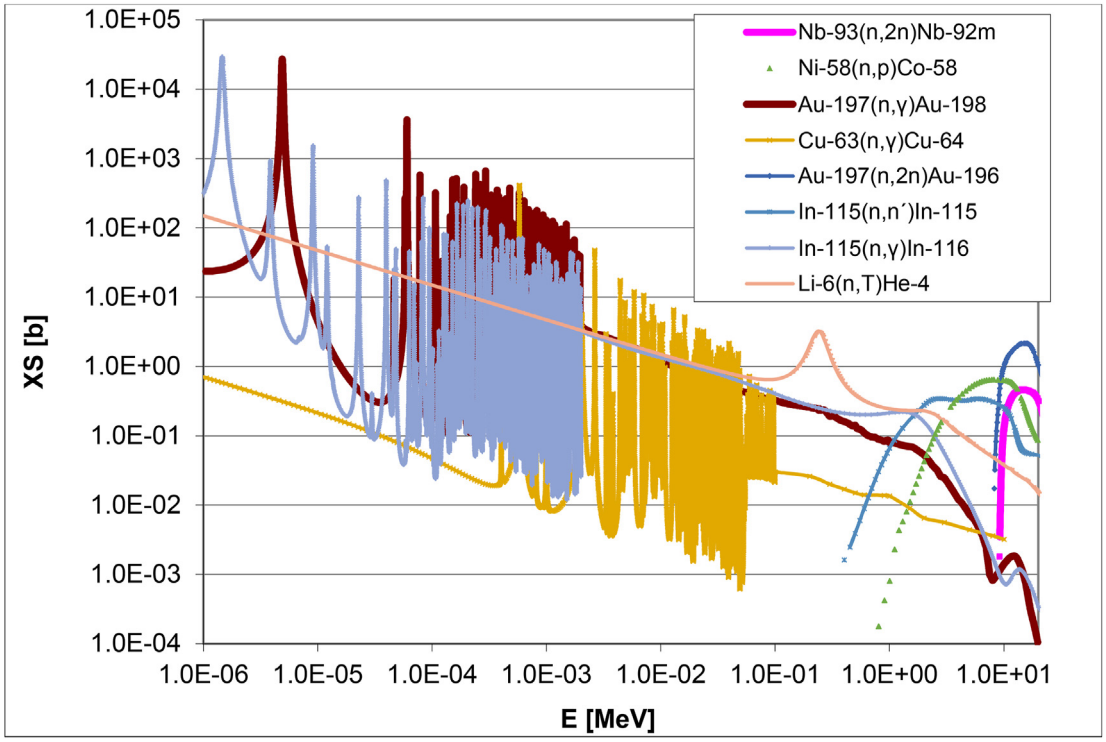

Fig. 3. Summary of dosimetric reactions cross sections taken from IRDFF-II library.

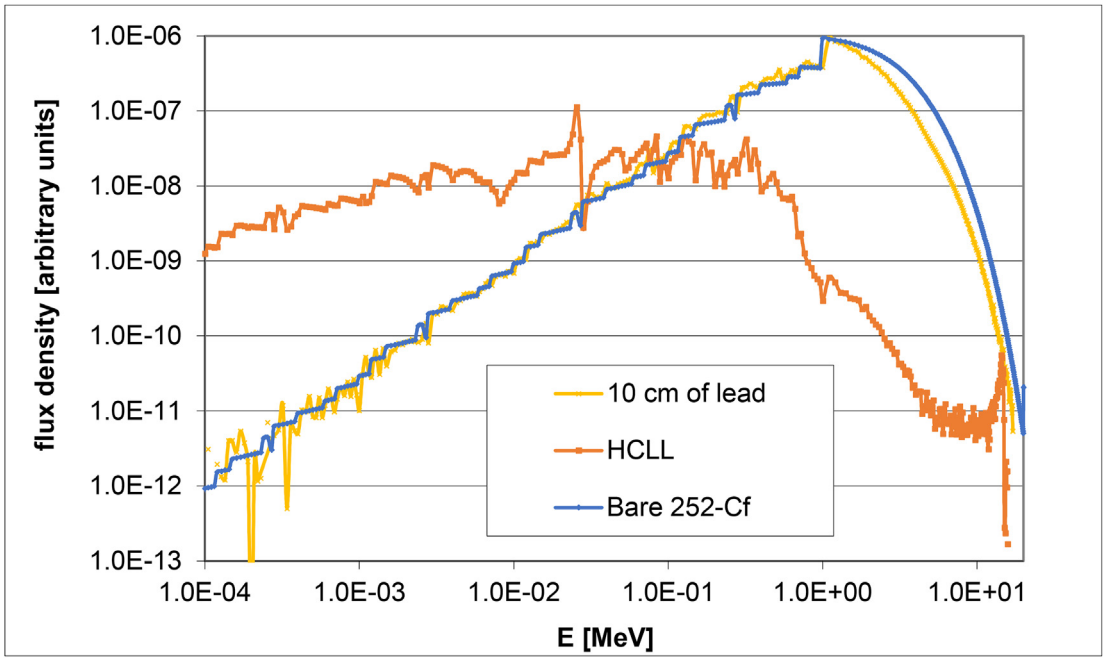

Fig. 4. Comparison of the calculated neutron spectra shapes.

in IRDFF-II library. These reactions were selected to cover broad range of neutron energies (1e-3 eV- 16 MeV), namely, ^{197}Au(n, 2n)^{196}Au, ^{58}Ni(n,p)^{58}Co, ^{93}Nb(n, 2n)^{92m}Nb, ^{115}In(n,n')^{115m}In, ^{115}In(n,γ)^{116m}In, ^{197}Au(n,γ)^{198}Au, and ^{63}Cu(n,γ)^{64}Cu reactions. The threshold reactions on niobium, and gold are sensitive in the high energy region, nickel and indium in the medium energy region and radiative capture reactions on copper, indium and gold are sensitive in the region under 0.1 MeV. All activation reactions used for evaluation were validated in the standard ^{252}Cf neutron spectrum, see Refs. [11,13–15,17]. Fig. 4 compares calculated neutron spectra in the place of activation foils (10 cm of lead) with the bare ^{252}Cf spectrum [12] and neutron spectrum inside the HCLL tritium breeding module. The spectra were multiplied by a constant to show shapes differences. The majority of neutrons inside the tritium breeding blanket will approximately be in the energy range of 1keV-1 MeV. HCLL spectrum was taken as a representative one

Table 4
Influence analysis.

Reaction	Antimony	Aluminium foil	^{204}Pb	^{206}Pb	^{207}Pb	^{208}Pb
^{197}Au(n,γ)^{198}Au	+0.50%	−0.27%	<0.1%	−0.33%	+0.22%	−0.69%
^{197}Au(n,2n)^{196}Au	+0.71%	−0.15%	<0.1%	+1.51%	+1.31%	+1.45%
^{63}Cu(n,γ)^{64}Cu	+0.35%	−0.38%	<0.1%	−0.35%	+0.17%	−0.06%
^{58}Ni(n,p)^{58}Co	−0.95%	−0.56%	<0.1%	−0.02%	−0.32%	+0.53%
^{93}Nb(n,2n)^{92m}Nb	−0.78%	−0.38%	<0.1%	+0.75%	−1.73%	−1.54%
^{115}In(n,n')^{115m}In	−0.91%	−0.51%	<0.1%	+0.34%	−0.21%	+0.80%
^{115}In(n,γ)^{116m}In	−0.20%	−0.32%	<0.1%	+0.02%	+0.31%	−0.01%

Table 5
Calculation and C/E−1 comparison for all reactions under study (ENDF/B-VIII.0 transport library).

Reaction	Lead thickness	Reaction rate [s^{-1} $atom^{-1}$]	C/E−1	Experimental Uncertainty
^{58}Ni(n,p)^{58}Co	10 cm	3.59E-29	+6.6%	3.2%
^{93}Nb(n,2n)^{92m}Nb	10 cm	1.83E-31	+2.9%	4.2%
^{197}Au(n,γ)^{198}Au	5 cm	3.31E-28	−15.8%	2.9%
^{197}Au(n,γ)^{198}Au	10 cm	1.24E-28	−51.4%	3.1%
^{197}Au(n,2n)^{196}Au	5 cm	6.48E-30	−0.5%	4.1%
^{197}Au(n,2n)^{196}Au	10 cm	1.19E-30	+2.4%	4.3%
^{63}Cu(n,γ)^{64}Cu	5 cm	3.83E-29	−1.1%	3.7%
^{115}In(n,n')^{115m}In	10 cm	8.52E-29	+0.2%	3.4%
^{115}In(n,γ)^{116m}In	10 cm	1.89E-28	−37.9%	3.1%

for the comparison and was calculated based on the information presented in Ref. [16]. The neutron spectra in the other lithium lead breed modules have a similar shape.

Table 4 summarizes the influence analysis of isotopic lead composition, thickness of the aluminium holder, and antimony content in lead bricks onto the final result. A conservative approach was employed in the analysis. That means that the reaction rates were calculated with minimal and maximal values of the studied parameter. A value with larger difference from nominal value was then taken into account. The Variance of the ^{204}Pb isotopic content was found negligible. Other isotopes have influence mainly for (n, 2n) reactions. The thin aluminium holder has influence at most 0.6% if omitted from geometry. The influence of antimony content is at most 1% for all reactions. This value was found as a difference between calculations containing 2.5% of antimony and pure lead.

Table 5 shows the results for 5 cm and 10 cm lead thickness and reaction rates comparisons for all reactions under study. The C/E is the ratio of the reaction rate calculated by MCNP6 and using IRDFF-II cross sections and the measured one. Generally, threshold reactions agree with calculation within 7%. However, for radiative capture reactions, the reasonable agreement is not the case. The only agreement within uncertainties is achieved for 5 cm of lead thickness and radiative capture reaction ^{63}Cu(n,γ)^{64}Cu. This reaction has an uncertainty of convolution of cross section with ^{252}Cf neutron spectrum equal to 8.41% in ^{252}Cf spontaneous fission neutron spectrum against ^{197}Au(n,γ)^{198}Au reaction which has an uncertainty of only 0.52%. As can be seen in Fig. 4, spectrum behind 10 cm of lead is not much different from pure ^{252}Cf, thus, one can expect similar uncertainties. The uncertainty behind the 10 cm of lead will not be much different. The comparison of neutron spectra for different scenarios is displayed in Fig. 4. The other capture reactions (In, Au) do not agree with calculation up to −51.43% for gold radiative capture reaction behind the 10 cm of lead. Table 6 shows computational reaction rates share distribution for different neutron energy regions for selected dosimetric reactions. The differences in the distribution between 5 cm and 10 cm of lead are negligible. The problematic region corresponds to the energies below 1 MeV since threshold reactions agree with the experiment and the total majority of share is above 1 MeV.

Table 7 shows the calculated reaction rate distribution of tritium production in the HCLL module, in pure ^{252}Cf neutron spectrum, and behind the 10 cm of lead. In the case of thicker lead, the mean energy of neutrons would be moved to lower energies. The total majority of tritium production in HCLL stems from neutrons below 1 MeV. Gold radiative capture has share of 40% in the energy range of 0.1 MeV−1 MeV, tritium production in HCLL has share of 16% in the same energy range. The gold radiative capture agreement is much better behind 5 cm of lead than 10 cm of lead. The disagreement behind 10 cm of lead is confirmed by In radiative capture. The share of 16% of total tritium production is non-

Table 7
^{6}Li(n,T)^{4}He reaction rate share for different neutron energy regions for different scenarios.

Energy range	HCLL	Pure^{252}Cf	10 cm of lead
1 MeV−16 MeV	0.02%	40.47%	26.80%
0.1 MeV−1 MeV	15.90%	56.15%	69.25%
1 keV-0.1 MeV	47.25%	3.35%	3.92%
1 meV-1 keV	36.83%	0.03%	0.03%

Table 6
Reaction rate share for different neutron energy regions in performed experiment.

Reaction	1 MeV−16 MeV	0.1 MeV−1 MeV	1 keV-0.1 MeV	1 meV-1 keV
^{197}Au(n,γ)^{198}Au	55.1%	40.3%	4.6%	0.0%
^{63}Cu(n,γ)^{64}Cu	33.7%	29.9%	26.6%	9.8%
^{115}In(n,n')^{115m}In	94.5%	5.5%	0.00%	0.0%
^{115}In(n,γ)^{116m}In	42.3%	51.0%	6.6%	0.0%

negligible amount. Substantial part of HCLL is composed of lead hence if the agreement is not achieved with 10 cm of lead. One can expect disagreement in case of larger thickness of lead and different value of tritium breeding ratio. Tritium breeding ratio value is crucial for the fusion reactor sustainability.

5. Conclusions

The performed experiment tested the ENDF/B-VIII.0 lead neutron transport library using the high emission standard ^{252}Cf neutron source. Generally, dosimetric threshold reactions agree with calculation reasonably well. Disagreement was found for radiative capture dosimetric reactions. These discrepancies are higher with thicker lead layers. It is important to validate the transport libraries with neutron spectra different from fusion spectrum. Thus the high emission ^{252}Cf neutron source can be used not only for validation in fission applications but equally also for fusion applications due to its low uncertainties. The cross sections are crucial for estimation of tritium breeding ratio. The ^{252}Cf isotropic source can be used for validation of some cross-sections important for fusion applications, i.e. reactions on structural materials, e.g. Cu, Pb, etc.

It would be useful to perform more experiments with different neutron spectra. Then it would be possible to deduce which energy regions are not well described by cross sections. However, there would still remain the problem of identifying the problematic isotopes.

Declaration of competing interest

The authors declare that they have no known competing financial interests or personal relationships that could have appeared to influence the work reported in this paper.

Acknowledgements

The presented work has been realized within Institutional Support by the Ministry of Industry and Trade and with the use of theinfrastructure Reactors LVR-15 and LR-0, which is financially supported by the Ministry of Education, Youth and Sports - project LM2015074, the SANDA project funded under H2020-EURATOM-1.1 contract 847552.

References

[1] J. Jordanova, U. Fischer, P. Pereslavtsev, Y. Poitevin, et al., Parametric neutronic analysis of HCLL blanket for DEMO fusion reactor utilizing vacuum vessel ITER FDR design, Fusion Eng. Des. 81 (19) (2006) 2213–2220.
[2] L.V. Boccaccini, G. Aiello, J. Aubert, C. Bachmann, T. Barrett, et al., Objectives and status of EUROfusion DEMO blanket studies, Fusion Eng. Des. 109–111 (Pt. B) (2016) 1199–1206.
[3] P. Batistoni, M. Angelone, U. Fischer, A. Klix, I. Kodeli, D. Leichtle, et al., Neutronics experiments for uncertainty assessment of tritium breeding in HCPB and HCLL blanket mock-ups irradiated with 14 MeV neutrons, Nucl. Fusion 52 (8) (2012), 083014.
[4] S. Kwon, M. Ohta, S. Sato, C. Konno, K. Ochiai, Lead benchmark experiment with DT neutrons at JAEA/FNS, Fusion Science andTechnology (2017) 362–367.
[5] K.J.R. Rosman, P.D.P. Taylor, Isotopic compositions of the elements, 1997, Pure Appl. Chem. 70 (1998) 217.
[6] T. Goorley, et al., Initial MCNP6 release overview, Nucl. Tech. 180 (2012) 298–315.
[7] M. Košťál, M. Schulc, et al., Validation of zirconium isotopes (n,γ) and (n,2n) cross sections in a comprehensive LR-0 reactor operative parameters set, Appl. Radiat. Isot. 128 (2017) 92–100.
[8] D.A. Brown, M.B. Chadwick, R. Capote, et al., ENDF/B-VIII.0.0: the 8th major release of the nuclear reaction data library with CIELO-project cross sections, new standards and thermal scattering data, Nucl. Data Sheets 148 (2018) 1–142.
[9] M.B. Chadwick, M. Herman, P. Obložinský, et al., ENDF/B-VII.1: nuclear data for science and Technology: cross sections, covariances, fission product yields and decay data, Nucl. Data Sheets 112 (2011) 2887–2996.
[10] A.J.M. Plompen, O. Cabellos, C. De Saint Jean, M. Fleming, A. Algora, M. Angelone, et al., The joint evaluated fission and fusion nuclear data library, JEFF-3.3, The European Physical Journal A 56 (7) (2020).
[11] A. Trkov, P.J. Griffin, S.P. Simakov, L.R. Greenwood, K.I. Zolotarev, R. Capote, et al., IRDFF-II: an updated neutron metrology library, Nucl. Data Sheets 163 (2020) 1–108.
[12] W. Mannhart, Status of the Evaluation of the Neutron Spectrum of ^{252}Cf(sf), in: IAEA Technical Report INDC(NDS)-0540, IAEA, Vienna, 2008. Presentation available at, www-nds.iaea.org/standards-cm-oct-2008/6.PDF.
[13] S. Manojlovic, A. Trkov, "Nuclear Cross Section Measurement Analysis in the Californium-252 Spectrum with the Monte Carlo Method", Conf, Nuclear Energy for New Europe, Ljubljana, Slovenia, 2011 contribution 307.
[14] W. Mannhart, Response of activation reactions in the neutron field of 252Cf(s.f, in: IAEA Technical Report Series No. 452, IAEA, Vienna, Austria, 2006, pp. 30–45.
[15] M. Schulc, M. Kostal, et al., Validation of IRDFF-II library by means of ^{252}Cf spectral averaged cross sections, Appl. Radiat. Isot. 155 (2020) 108937.
[16] J.-C. Jaboulay, G. Aiello, J. Aubert, A. Morin, M. Troisne, Nuclear analysis of the HCLL blanket for the European DEMO, Fusion Eng. Des. 124 (November 2017) 896–900.
[17] M. Schulc, M. Kostal, R. Capote, et al., Validation of selected (n,2n) dosimetry reactions in IRDFF-1.05 library, Appl. Radiat. Isot. 143 (2019) 132–140.
[18] M. Schulc, M. Kostal, et al., Application of ^{252}Cf neutron source for precise nuclear data experiments, Appl. Radiat. Isot. 151 (2019) 187–195.